

Inelastic Scattering of He³ Ions at Intermediate Energies*

E. F. GIBSON,† J. J. KRAUSHAAR, B. W. RIDLEY,‡ AND M. E. RICKEY§
Department of Physics and Astrophysics, University of Colorado, Boulder, Colorado

AND

R. H. BASSEL||
Oak Ridge National Laboratory, Oak Ridge, Tennessee
 (Received 24 October 1966)

The inelastic scattering of He³ ions from Ca⁴⁰, Fe⁵⁶, and Ni⁵⁸ has been studied at a bombarding energy of 37.7 MeV, and the scattering from Y⁸⁹ and Zr⁹⁰ has been investigated using 43.7-MeV He³ ions. The distorted-wave theory, using the optical parameters derived previously, gave an adequate description of the data on the collective model, provided both real and imaginary potentials were assumed to be deformed. Angular-momentum transfers and deformation parameters are in general agreement with those obtained from other experiments.

I. INTRODUCTION

IN the preceding paper the results of the elastic scattering of 37.7- and 43.7-MeV He³ ions from a number of medium-weight nuclei were described. This paper is concerned with inelastic He³ scattering from the same nuclei.

Inelastic charged-particle scattering has been rather extensively studied in the past few years, particularly using protons, deuterons, and alpha particles. These studies have yielded a considerable amount of information of the reaction mechanism and the energy of excited states as well as spin assignments and deformation parameters for a more limited number of states. Inelastic He³ scattering has, on the other hand, not been studied to any extent. When this work was initiated only one limited experimental study¹ of inelastic He³ scattering had been made. The He³ particle is a strongly interacting particle similar to the alpha particle but differs in that it has a spin and isobaric spin of $\frac{1}{2}$. For this reason one would expect important differences in the excitation by He³ and alpha particles of certain states, particularly those of unnatural parity.²

The analysis presented in this paper is based upon the distorted wave theory and the collective model of nuclear structure. The theory has been discussed in detail elsewhere.³ Here we briefly recapitulate the main ideas and the extensions to the inelastic scattering of He³ ions.

On this model the potential responsible for the scat-

tering is assumed to be deformed or deformable. If coupling between the elastic channel and the inelastic channels is weak then the interaction responsible for first-order transitions (single excitations) is proportional to the radial derivative of the optical potential for elastic scattering. Thus, once the parameters for elastic scattering are known, the inelastic angular distributions are determined except for over-all normalizations. This normalization, β^2 , (or $\beta^2 R^2$) is just the mean-square deformation of the target ground state due to zero-point oscillations. If the collective model is indeed applicable, the values of the deformation parameter β (or the deformation length βR) deduced from these experiments should be comparable to the values found by other means, such as the scattering of other projectiles or from Coulomb excitation.

Straightforward application of the collective-model ideas suggest that the interaction should be complex, i.e., that the imaginary part of the potential, as well as the real part, follows the motion of the nucleus. Such an extension has been shown to yield important improvements in the description of the inelastic scattering of nucleons⁴ and alpha particles⁵ and to be essential to the description of the inelastic scattering of deuterons and He³ ions.^{6,7} The necessity for this modification in the present case is discussed below.

The purpose of the present work lies less in elucidating new nuclear spectroscopic information than as a study of the applicability of the distorted-wave theory and the collective model to the scattering of He³ ions, and in the usefulness of He³ as a spectroscopic tool.

II. EXPERIMENTAL PROCEDURES AND DATA ANALYSIS

The experimental apparatus has been described in the previous paper. Only those procedures not discussed

⁴ M. P. Fricke and G. R. Satchler, *Phys. Rev.* **139**, B567 (1965).

⁵ H. W. Broek, J. L. Yntema, B. Buck, and G. R. Satchler, *Nucl. Phys.* **64**, 259 (1965).

⁶ J. K. Dickens, F. G. J. Perey, and G. R. Satchler, *Nucl. Phys.* **73**, 529 (1965).

⁷ E. R. Flynn and R. H. Bassel, *Phys. Rev. Letters* **15**, 168 (1965).

* Research sponsored by the U. S. Atomic Energy Commission under contract with the Union Carbide Corporation and the University of Colorado.

† Present address: University of Oregon, Eugene, Oregon.

‡ Permanent address: Atomic Energy Research Establishment, Harwell, England.

§ Present address: University of Indiana, Bloomington, Indiana.

|| Present address: Brookhaven National Laboratory, Upton, New York.

¹ J. Aguilar, W. E. Burcham, J. B. A. England, A. Garcia, P. E. Hodgson, P. V. March, J. S. C. McKee, E. M. Mosinger, and W. T. Toner, *Proc. Roy. Soc. (London)* **A257**, 13 (1960).

² W. W. Eidson and J. G. Cramer, Jr., *Phys. Rev. Letters* **9**, 497 (1962).

³ R. H. Bassel, G. R. Satchler, R. M. Drisko, and E. Rost, *Phys. Rev.* **128**, 2693 (1962).

TABLE I. Optical-model parameters used in distorted-wave calculations.

Target	E (MeV)	V_0 (MeV)	r_0 (F)	a (F)	W_0 (MeV)	r_0' (F)	a' (F)	χ^2
Ca^{40}	37.7	176.92	1.14	0.723	14.53	1.64	0.91	1456
Fe^{56}	37.7	174.2	1.14	0.723	16.8	1.60	0.81	1267
Ni^{58}	37.7	172.65	1.14	0.723	16.2	1.60	0.81	600
Y^{89}	43.7	171.39	1.15	0.724	14.97	1.61	0.80	4579
Zr^{90}	43.7	174.9	1.13	0.7355	16.53	1.58	0.79	513

there are mentioned here. The Q values were determined from the number of channels between the ground- and excited-state peaks, using one or more prominent isolated states of well-known excitation in the same target to establish the energy scale. For Y^{89} , whose levels are relatively close, the energy calibrations had to be made with a CH_2 target using scattering for the ground, 4.433-, 7.656-, and 9.62-MeV states of C^{12} . Q values determined in this work represent the average of determinations at several different angles, after kinematic and target-thickness corrections had been made. The uncertainties are estimated to be ± 25 keV for strongly excited states and ± 50 keV for the weaker ones.

The distorted-wave calculations were primarily carried out using the computer program JULIE, although some were made using a preliminary version of a distorted-wave code written by P. D. Kunz.

The deformation parameters β were obtained by renormalizing the calculated angular distributions to fit the data, and are estimated to be uncertain within 10% of the quoted values.

III. RESULTS

A. General Discussion

Numerous excited states were seen in the inelastic scattering of He^3 from the targets studied. The Q values of these excited states were calculated for all states which were observed at enough angles to make their identification positive. However, angular distributions are shown only for states for which the data were precise and complete enough to give meaningful comparisons to theory.

Missing portions in the inelastic angular distributions arise for two reasons. Either the peak was very weak and could not be identified in the spectrum, or the peak due to elastic scattering of He^3 from a light impurity nucleus had coalesced with the peak of interest.

He^3 inelastic-scattering angular distributions generally appear to have more pronounced structure than is the case for proton scattering, making them useful for angular-momentum transfer determinations. The angular distributions obey the Blair phase rule⁸ reasonably well but are seldom seen to be exactly in or out of phase with elastic-scattering distributions. The angular distributions corresponding to the ground state, the

2^+ state, at 0.85 MeV and to the 3^- state at 4.52 MeV of Fe^{56} are shown in Fig. 1. The $L=2$ distribution is seen to be nearly, but not exactly, out of phase with the elastic; similarly the $L=3$ distribution is nearly, but not exactly, in phase with the elastic. The $L=2$ and $L=3$ distributions are closer to being out of phase than the elastic and the $L=2$ distribution.

Many optical-model parameter sets have been shown in the preceding paper to fit the elastic scattering of He^3 . Of these, the set with a real potential-well depth U_0 near to 180 MeV was chosen as a basis for the analysis of inelastic scattering for reasons discussed in that paper. However, the effect of using other parameter sets that minimize χ^2 for elastic scattering has been

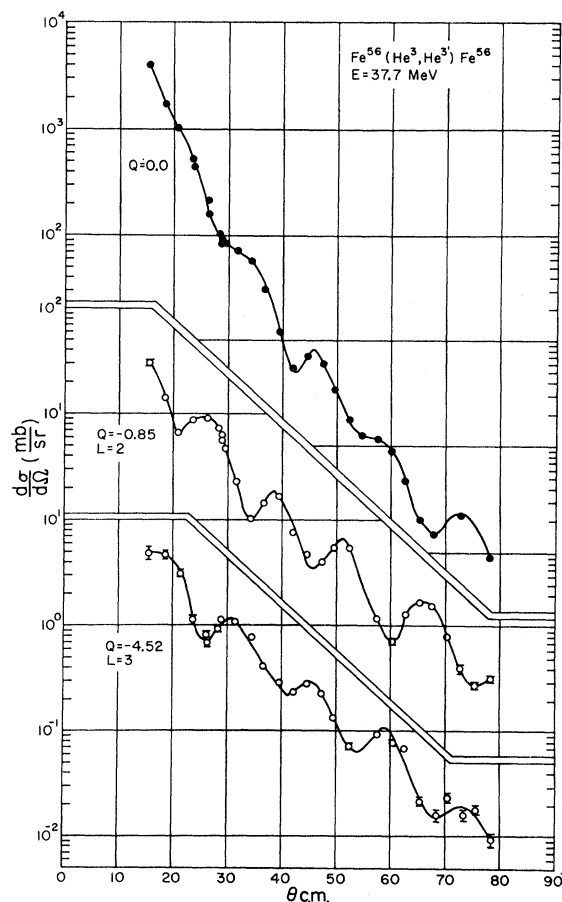


FIG. 1. Angular distributions for the elastic and two inelastic groups from Fe^{56} . The solid lines, which were drawn through the data points, are to show the phase relationships of the oscillations.

⁸ J. S. Blair, Phys. Rev. **115**, 928 (1959).

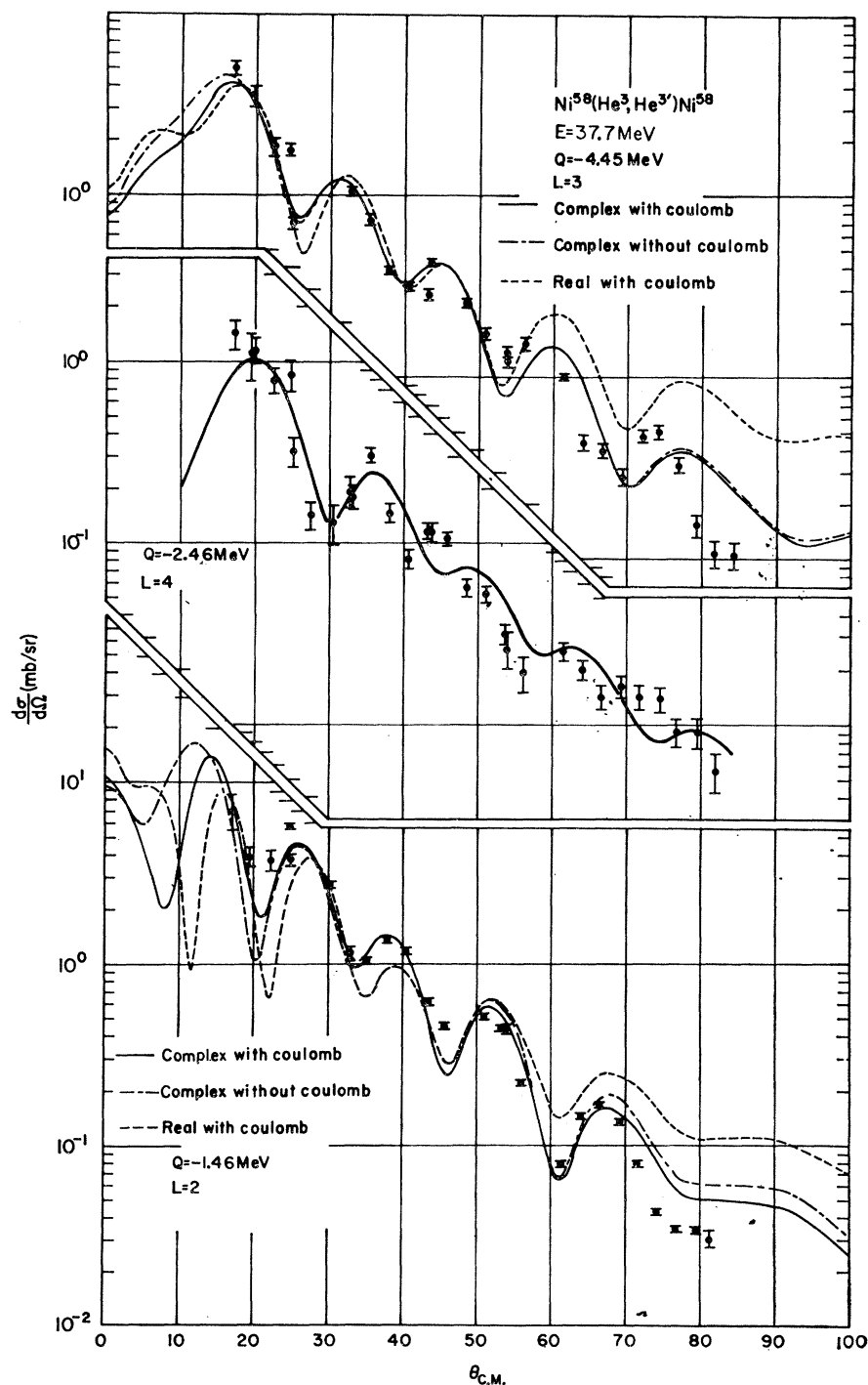


FIG. 2. Angular distributions for three states of Ni^{58} . The solid and dashed lines are theoretical distorted-wave predictions under the various conditions.

studied for two angular distributions, and these results will be discussed below. The parameter values used are given in Table I and are the standard parameters of the previous paper except in the case of Y^{89} and Zr^{90} , where the parameters vary only slightly from the standard parameters and were used in the distorted wave code before the choice of the standard parameters was made. The need to use a complex coupling inter-

action rather than a purely real one was also investigated in some detail for a limited number of cases before proceeding to examine the major part of the results. In the calculations with a complex interaction, the deformations of the real and imaginary parts of the potential were assumed to be the same.

In Fig. 2 are shown distorted-wave-calculated cross sections for the first 2^+ state of Ni^{58} for both real and

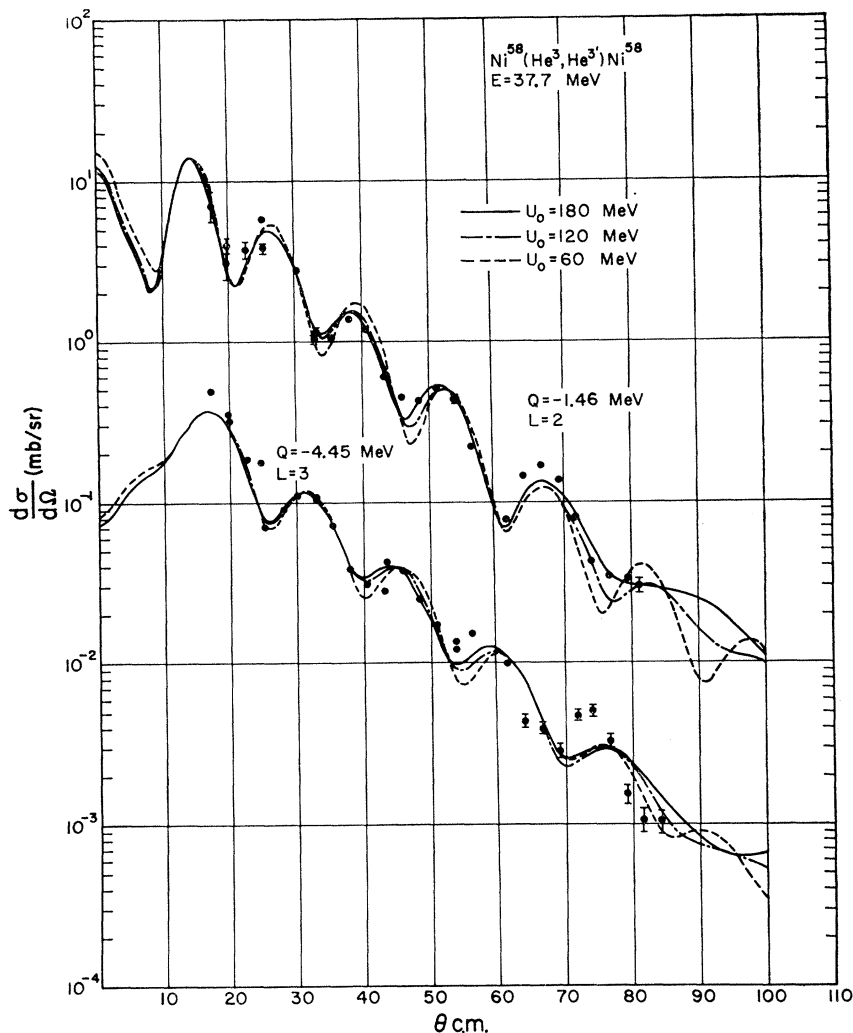


FIG. 3. Comparison of the distorted-wave predictions calculated using real potential depths that corresponded to minima in χ^2 of the set-II parameters discussed in the previous paper.

complex interactions. The real interaction prediction does not fit the data nearly as well as does the complex interaction. The theoretical angular distribution based on the real interaction does not decrease as fast as the data with increasing scattering angle. The distribution calculated using the complex interaction, however, fits the data quite well. Its oscillations are more nearly in phase with the data and it decreases with angle at approximately the same rate as the data. Also shown in Fig. 2 are the experimental and theoretical angular distributions for the strongly excited 3^- state at 4.45 MeV. Here again the complex interaction clearly gives a better fit to the data than does the real, particularly at angles greater than 50° .

Not only is the fit obtained using the complex interaction better than that of the real interaction, but the distortion parameter, β , calculated by comparing the predicted and experimental distributions agrees better with other data. The distortion parameter calculated from the real interaction for this $L=2$ state in Ni^{58} at 1.46 MeV is 0.32, and the value obtained for the

complex interaction is 0.12. The values of β calculated for this state in other experiments^{5,7,9,10} range from 0.15 to 0.18. This indicates that the imaginary part of the interaction gives the major contribution to the calculated scattering cross section, since the cross section calculated using the complex interaction is about 7 times as large as that using the real interaction. Similarly, the value of β obtained for the $L=3$ excitation of the 4.45-MeV state is 0.12 for the complex interaction and 0.26 for the real. Other experiments^{5,7,9,10} have given values of β for this state of 0.10 to 0.19.

Similar results were obtained in comparing the real and complex interactions in the case of the lowest-lying 3^- state of Ca^{40} .¹¹ In the case of Fe^{56} the real fit appeared better but the distortion β predicted was again too large. These results also agree rather well with those of

⁹ G. R. Satchler, Nucl. Phys. **70**, 177 (1965).

¹⁰ P. Darrulat, G. Igo, H. G. Pugh, J. M. Meriwether, and S. Yamabe, Phys. Rev. **134**, B42 (1964).

¹¹ E. F. Gibson, J. J. Kraushaar, and M. E. Rickey, Bull. Am. Phys. Soc. **10**, 539 (1965).

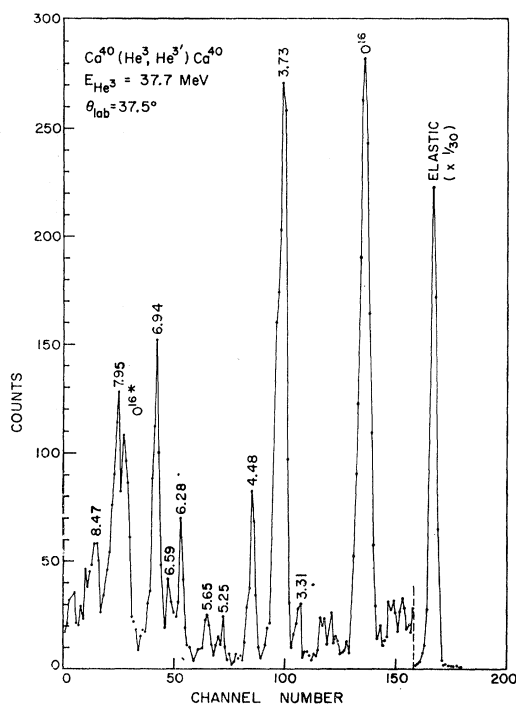


FIG. 4. An energy spectrum of 37.7-MeV He^3 ions scattered by Ca^{40} .

Flynn and Bassel⁷ derived from 22-MeV He^3 scattering from Ni^{58} , Fe^{56} , and Fe^{58} .

In the above calculations, Coulomb excitation was included. Figure 2 also shows the effect of excluding the Coulomb excitation in the distorted-wave calculations. Except for angles less than 20° its effects are quite small although it generally improves the agreement with the data.

In the distorted-wave calculations in the remainder of this paper, unless noted, a complex interaction will be used, and Coulomb excitation will be included for angular-momentum transfers of $L=2$ and $L=3$.

Distorted-wave calculations were made for the first $L=2$ and $L=3$ states of Ni^{58} using various optical-model potentials which gave equally good fits to the elastic scattering angular distribution. These potentials correspond to minima in χ^2 of the set-II parameters discussed in the previous paper. The potentials used are given in Table II. The fits to the data using these various potentials are shown in Fig. 3. Generally, the theoretical angular distributions are quite similar for the three potentials for both the $L=2$ and $L=3$ excita-

TABLE II. Optical-model parameters used for the distorted-wave calculations with Ni^{58} at 37.7 MeV to examine the dependence of the angular distributions on U_0 .

U_0 (MeV)	r_0 (F)	a (F)	W_0 (MeV)	r_0' (F)	a' (F)
180	1.11	0.724	18.28	1.60	0.810
120	1.89	0.720	16.96	1.60	0.810
60	1.37	0.670	15.64	1.60	0.810

tions. It is apparent, however, that the 180-MeV potential gives a better fit to the experimental data, particularly in the $L=2$ case.

B. Results with Ca^{40}

A typical energy spectrum of He^3 scattered by Ca^{40} is shown in Fig. 4. The energy resolution is about 100 keV. The ground and 4.48-MeV states were used to establish the energy scale. The major contaminants in this target were found from their kinematic behavior to be oxygen and, to a lesser extent, carbon.

Angular distributions for the states at 3.73, 4.48, 6.29, 6.59, and 6.94 MeV are shown in Fig. 5. The error bars indicate relative errors only. The solid curves are distorted-wave predictions for the angular-momentum transfers shown in the figure using a collective-model interaction with a complex potential.

The 3.73-MeV state is slightly broader on the high-energy side than the elastic peak because of the unresolved 3.90-MeV state. These states are known to be 3^- and 2^+ , respectively, from other work. The contribution of the 3.90-MeV state to the peak was found by Gaussian decomposition to be less than 10% at most angles. However, near 40° where the 3^- state gives a minimum in cross section and where the 2^+ state should be at a maximum, the contribution of the 2^+ state is about 35%. The distorted-wave prediction for the 3.73-MeV state with $L=3$ agrees with the data except near the minima.

The 4.48-MeV state is the well-known 5^- state¹² of Ca^{40} . The angular distribution predicted by the distorted-wave theory is in good agreement with the experimental distribution for this state.

The theoretical distribution for an $L=3$ transition corresponds well with the angular distribution for excitation of the 6.29-MeV state, in good agreement with other results.¹³ An $L=3$ transition also compares reasonably with the distribution for the state at 6.59 MeV, in agreement with the assignments of others.¹⁴

The strong peak at 6.94 MeV is seen in the spectrum to be broader than the elastic peak. Three states were seen in this region by Grace and Poletti¹³ at 6.91, 6.93, and 6.95 MeV, one of which they determined to be a 2^+ state. Comparing distorted-wave predictions corresponding to different values of angular-momentum transfer, an $L=2$ transition was found to correspond well with the data, with an improvement made by adding some $L=3$ contribution. Adding in various amounts of $L=1$ did not improve the comparison. The $L=1$ curve by itself is obviously not in agreement with this data. Gray *et al.*¹⁴ also obtained agreement with proton-

¹² *Nuclear Data Sheets*, compiled by K. Way *et al.* (Printing and Publishing Office, National Academy of Sciences—National Research Council, Washington 25, D.C.).

¹³ M. A. Grace and A. R. Poletti, *Nucl. Phys.* **78**, 273 (1966) and references contained therein.

¹⁴ W. S. Gray, R. A. Kenefick, and J. J. Kraushaar, *Nucl. Phys.* **67**, 542 (1965) and references contained therein.

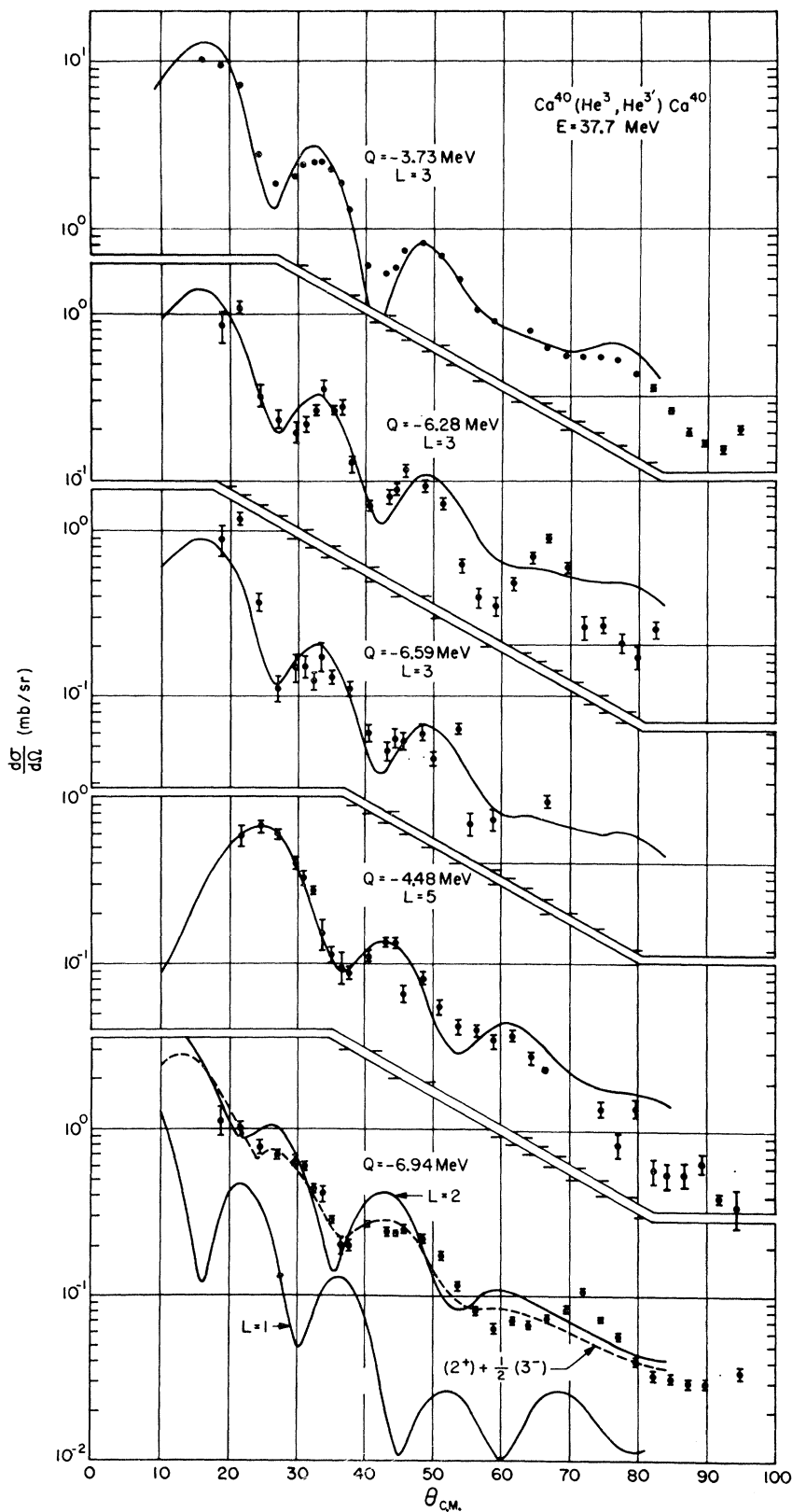


FIG. 5. Experimental and theoretical angular distributions for Ca^{40} . The $L=1$ distorted-wave curve for the state at 6.94 MeV is arbitrarily displaced from the data for purposes of clarity.

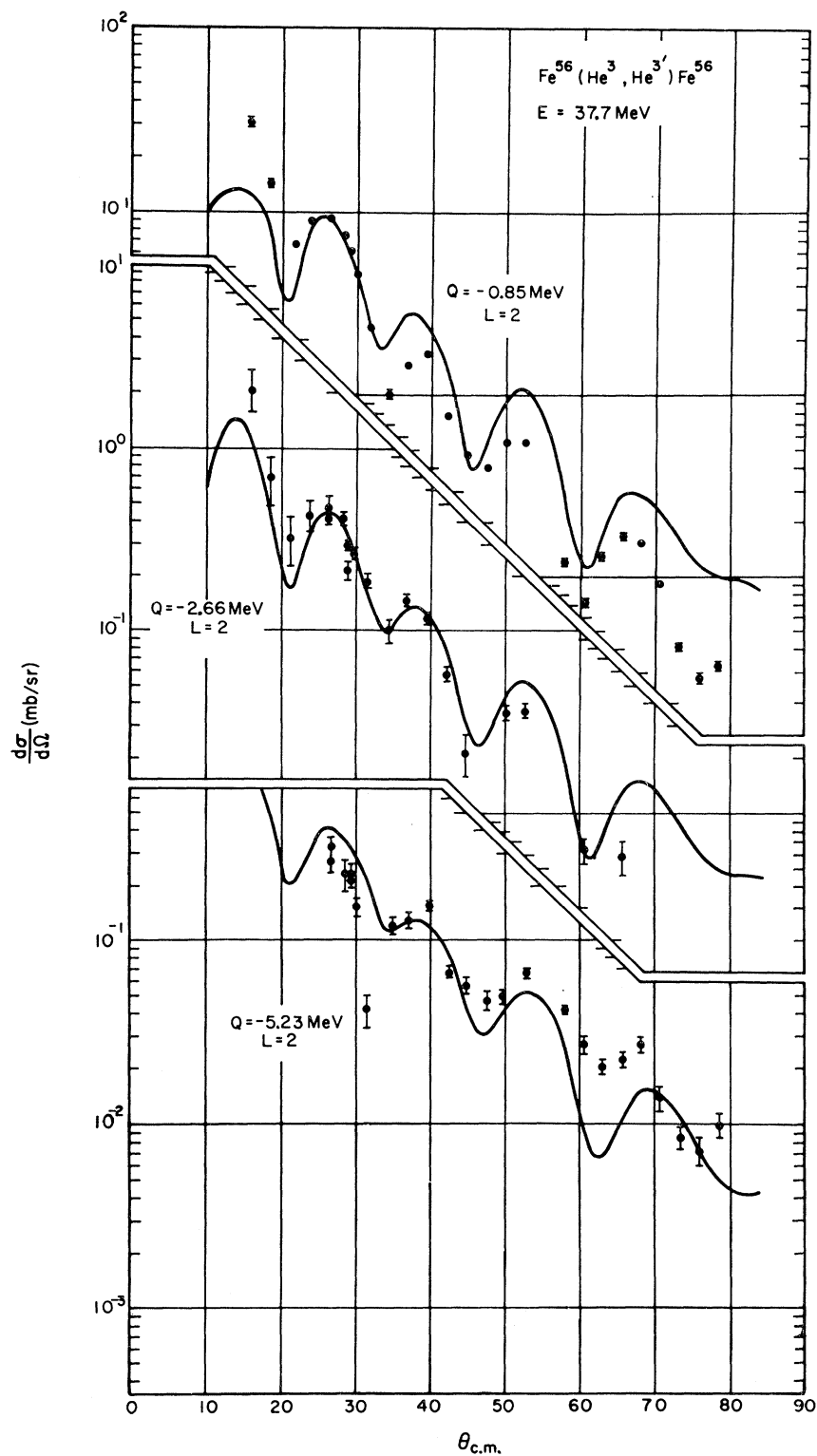


FIG. 6. Experimental and theoretical angular distributions for three $L=2$ states in Fe^{56} .

scattering data for this state with an $L=2$ transition. Springer¹⁵ in his α -particle scattering data from Ca^{40} found that a combination of $L=2$ and 3, was preferred

¹⁵ A. Springer and B. G. Harvey, Phys. Letters 14, 116 (1965).

over $L=1$ and 2. However, Kossler *et al.*¹⁶ found good agreement to their $(\alpha, \alpha'\gamma)$ angular-correlation data with

¹⁶ W. J. Kossler and K. Nogatani, Bull. Am. Phys. Soc. 11, 81 (1966).

a single $L=1$ state. Bauer *et al.*¹⁷ have also made a 1^- assignment to this state from inelastic α -particle scattering. The reason for this discrepancy is unknown.

In addition to the states discussed above, states at 3.31, 5.25, 5.65, 5.94, 7.95, and 8.47 MeV were observed to be excited, but the angular distributions were inadequate to justify further analysis.

C. Results from Fe⁵⁶

A typical spectrum of 37.7-MeV He³ scattered from Fe⁵⁶ was shown in the previous paper. The three strong states at 0.845, 2.66, and 4.52 MeV were used to calculate the conversion gain which was subsequently used to determine the Q values for the other states.

The angular distributions for the states at 0.85, 2.66, and 5.23 MeV are shown in Fig. 6. The 0.85- and 2.66-MeV states are well known to be 2^+ states.¹² The distorted-wave predictions for angular-momentum transfer $L=2$ have the correct phase and general shape to fit both the 0.85- and 2.66-MeV experimental data, although for the 0.85-MeV state, the average cross sections at large angles are lower than predicted. Judging from the distorted-wave fit, the state at 5.23 MeV probably is also a 2^+ state.

The angular distribution for the 3^- state¹⁸ at 4.52 MeV shown in Fig. 7 is fitted well by the theory. However, that for the 4^+ state^{19,20} at 2.06 MeV, also shown in this figure, is poorly fitted by the DW theory in which only single excitation processes are considered. A similar situation arises in excitation of the corresponding 4^+ state in Ni⁵⁸ and this will be discussed in Sec. D.

States were also observed to be excited at energies of 3.12, 3.38, 4.10, and 6.77 MeV, but are not discussed here because either the angular distributions were of poor quality or the states have been found in other work to be multiplets.

D. Results from Ni⁵⁸

A large number of states were seen in Ni⁵⁸ up to 7.5-MeV excitation. A typical spectrum is shown in Fig. 8. The conversion gain was determined using the 1.46- and 2.46-MeV states. The energy resolution was generally about 175 keV (full width at half-maximum, FWHM).

The He³ inelastic angular distributions for excitation of the well-known levels of Ni⁵⁸ at 1.46, 2.46, and 4.45 MeV are shown in Fig. 2. The 1.46- and 4.45-MeV states are the well known 2^+ and 3^- states,¹² both of which are fitted well by the distorted-wave theory using a complex interaction, as discussed earlier.

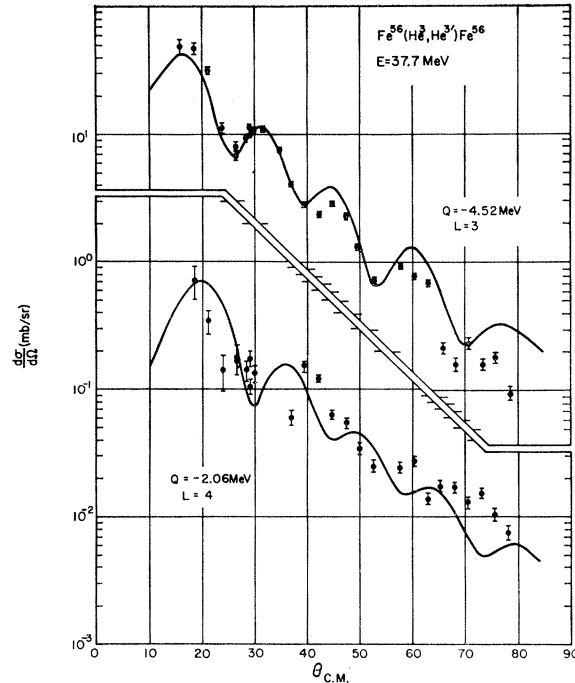


FIG. 7. Experimental and theoretical angular distributions for Fe⁵⁶.

According to the Blair phase rule for single excitations in the inelastic scattering of strongly absorbed particles, the angular distributions corresponding to even values of angular-momentum transfer should be out of phase, and those corresponding to odd values of angular-momentum transfer should be in phase with the elastic-scattering angular distribution. The 2.46-MeV state is known to be a 4^+ state.¹² Ignoring the solid curves in Fig. 2, it can be seen that the phase of the 2.46-MeV distribution is between that of the 2^+ and 3^- states, but is nearer that of the 3^- state, in disagreement with the Blair phase rule for single excitations but in agreement with other results on alpha-particle scattering.^{21,22} The single excitation, $L=4$ distorted-wave curve is shown with the data for the state at 2.46 MeV. The maxima and minima occur at too large angles becoming worse with increasing scattering angle, until it is entirely out of phase at 45° .

Buck,²³ considering the above state of Ni⁵⁸ and 40-MeV alpha-particle scattering showed that this discrepancy with the Blair phase rule can be explained if the transition is a combination of multiple (double) excitation and a direct two-phonon excitation. This argument presumably would also apply to excitation of this 4^+ state by He³, and to excitation of the corresponding 4^+ state in Fe⁵⁶ discussed previously. There is

¹⁷ R. W. Bauer, A. M. Bernstein, G. Heymann, E. P. Lippincott, and N. S. Wall, Phys. Letters **14**, 129 (1965); E. P. Lippincott, thesis, Massachusetts Institute of Technology, 1966 (unpublished).

¹⁸ K. Matsuda, Nucl. Phys. **33**, 536 (1962).

¹⁹ O. J. Poppema, J. G. Siekman, R. Van Wageningen, and H. A. Tolhoek, Physica **21**, 223 (1955).

²⁰ A. N. Diddens, W. J. Huiskamp, J. C. Severiens, A. R. Miedema, and M. J. Steenland, Nucl. Phys. **5**, 58 (1958).

²¹ R. Beurtey, P. Catillon, R. Chaminade, M. Crut, H. Faraggi, A. Papineau, J. Saudinos, and J. Thirion, Compt. Rend. **252**, 1756 (1961).

²² H. W. Broek, T. H. Braid, J. L. Yntema, and B. Zeidman, Phys. Rev. **126**, 1514 (1962).

²³ B. Buck, Phys. Rev. **127**, 940 (1962).

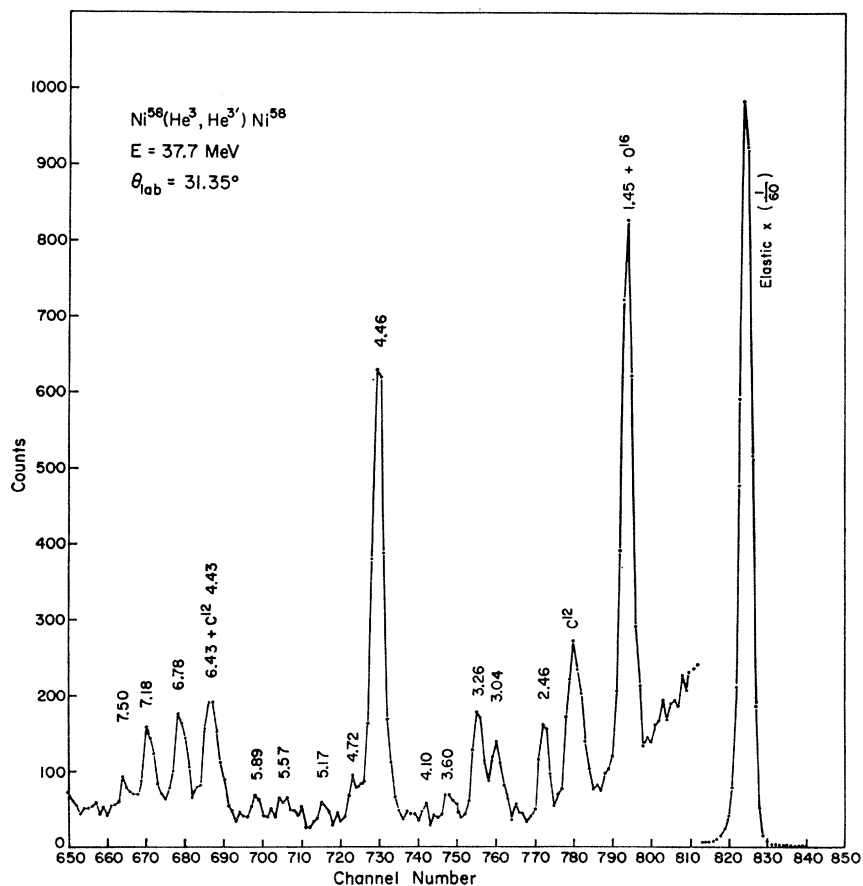


FIG. 8. An energy spectrum of 37.7-MeV He^3 ions scattered from Ni^{58} .

evidence however that the 2.46-MeV state is a doublet,²⁴ with energies of 2.456 and 2.483 MeV. It is therefore possible, if the two members of the doublet are excited with comparable cross sections, that the conclusions drawn concerning the angular distributions are incorrect since the doublet was not resolved.

The angular distributions of the 3.04- and 3.26-MeV states are seen in Fig. 9 to be almost identical and agree relatively well with an $L=2$ prediction, as has been suggested by others.^{9,25} The angular distribution for the state at 4.72 MeV is out of phase with the elastic as are all of the distributions in Fig. 9. The distorted-wave curve corresponding to an $L=4$ transition agrees well with the data for this state. The angular distributions from the states at 3.60 and 5.57 MeV, also shown in Fig. 9, are quite similar in shape and both are out of phase with the elastic distribution. However, neither an $L=2$ nor 4 curve gives a very good fit, the $L=4$ being the better of the two for angles greater than 30° .

Three relatively strong peaks at 6.78, 7.18, and 7.50 MeV were seen, but the angular distributions contain little structure. All three appear to be in phase with the

elastic distribution, in agreement with the results of Broek *et al.*²² for the 6.8- and 7.1-MeV states.

Other states were seen to be excited at 3.88, 4.10, 5.17, 5.89, 6.23, and 6.43 MeV, but are not discussed here because the angular distributions were poor.

E. Results from Y^{89}

A typical spectrum of He^3 ions scattered from Y^{89} is shown in Fig. 10. The data for this nucleus were of poorer quality than for the others, mainly because of major impurities in the target (carbon, oxygen, and $A \approx 175$), and the large energy width per channel. Therefore it was considered less from the viewpoint of spectroscopy than as a supplement to recent nuclear-structure studies of Y^{89} made with protons and alpha particles.

The Y^{89} nucleus may be considered as a Sr^{88} core plus a proton, a $p_{1/2}$ state, or as a Zr^{90} core and a proton hole in the $p_{1/2}$ shell. Considering the excited states of Y^{89} as arising from core excitations with the proton coupled weakly to the core, two states in Y^{89} would be expected corresponding to each excited state of the core, one with $J_1 = L - j = L - \frac{1}{2}$ and one with $J_2 = L + j = L + \frac{1}{2}$, where J is the total angular momentum of the nucleus, L is the orbital angular-momentum transfer,

²⁴ R. R. Spencer, G. C. Phillips, and T. E. Young, Phys. Rev. **108**, 69 (1957).

²⁵ H. Crannell, R. Helm, H. Kendall, J. Oeser, and M. Yearian, Phys. Rev. **123**, 923 (1961).

and j is the angular momentum of the additional particle outside the core. The ratio of the cross sections for the two states arrived at in this way should be equal to the ratio of their statistical weights, or

$$\frac{d\sigma_1}{d\sigma_2} = \frac{2J_1+1}{2J_2+1} = \frac{L}{L+1}.$$

The sum of the cross sections to the multiplet states in the odd A nucleus should be equal to the cross section

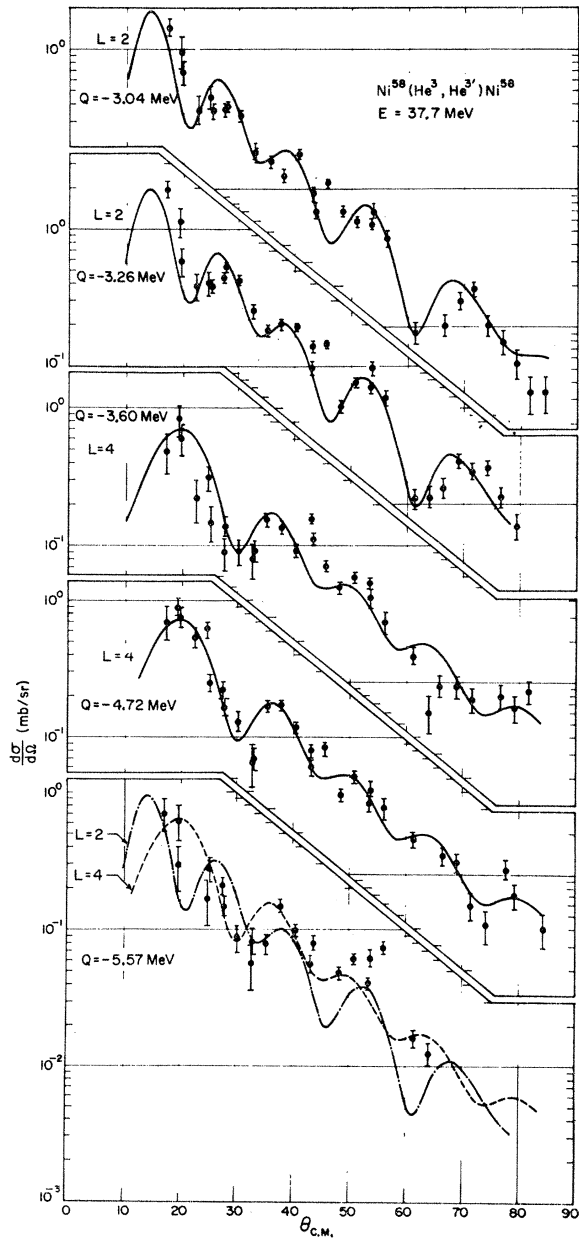


Fig. 9. Experimental and theoretical angular distributions for Ni⁵⁸.

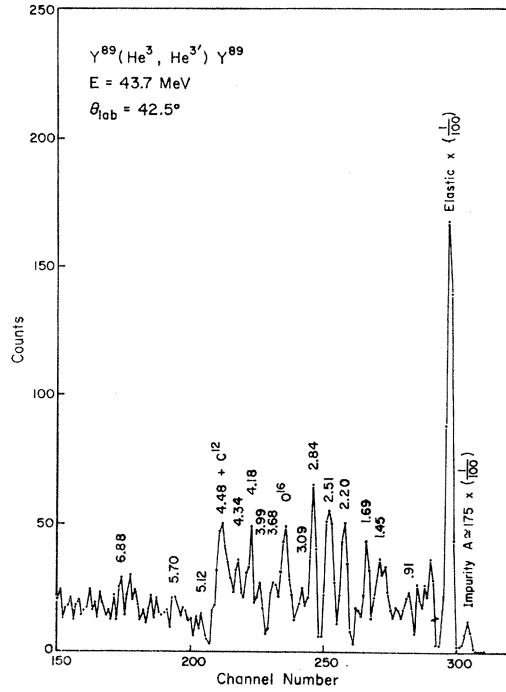


Fig. 10. An energy spectrum of 43.7-MeV He³ ions scattered from Y⁸⁹.

to the corresponding state of the core nucleus, or

$$\frac{d\sigma}{d\Omega}(0 \rightarrow E_c) = \sum_{i=1}^{2j+1} \frac{d\sigma}{d\Omega}(0 \rightarrow E_i),$$

where E_c is the core-state energy and E_i the energies of the corresponding multiplet states of the odd- A nucleus.

According to the center-of-gravity theorem of Lawson and Uretsky,²⁶ the separation of the center-of-gravity energy of the multiplets in the odd- A nucleus should be identical to the separation between the corresponding states in the even-even core nucleus. The center-of-gravity energy of the multiplets is given in the case of $j = \frac{1}{2}$ by

$$E_{cg} = \frac{(2J_1+1)E_1 + (2J_2+1)E_2}{2(2J_c+1)} = E_c.$$

The states corresponding to excitations of the $L=2$ state at 1.84 MeV and the $L=3$ state at 2.74 MeV in the Sr⁸⁸ core are of interest here. According to the above theory the ratio of the cross sections in Y⁸⁹ for the states corresponding to angular-momentum transfer $L=2$ should be $\frac{2}{3}$ and the ratio for the two $L=3$ cross sections should be $\frac{3}{4}$. Figure 11 shows the cross sections for the states at 1.45 and 1.69 MeV with theoretical angular distributions for $L=2$ transitions. The distorted-wave curves here are used to determine the dis-

²⁶ R. D. Lawson and J. L. Uretsky, Phys. Rev. **108**, 1300 (1957).

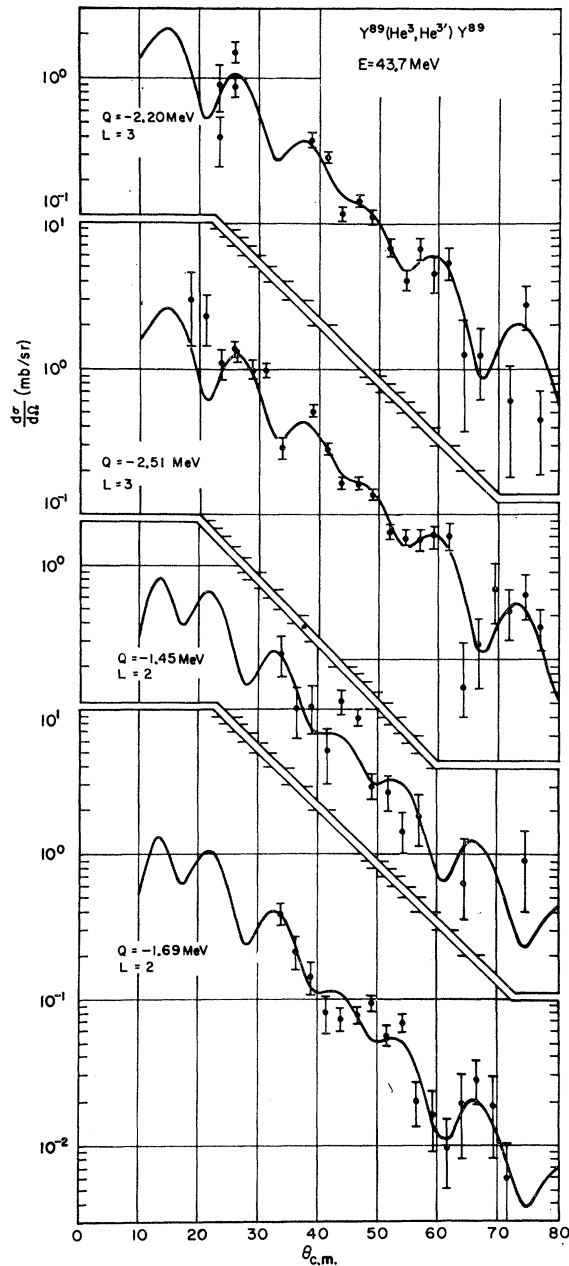


FIG. 11. Experimental and theoretical angular distributions for the four low-lying states of Y^{89} for which core excitation is considered in the text.

tortion parameters and are not intended to be used to determine the angular-momentum transfer, which has been well determined by other experiments.²⁷⁻²⁹ The ratio of the cross sections of the 1.45- and 1.69-MeV states is found here to be 0.62 ± 0.08 , in good agreement

²⁷ M. M. Stautberg, J. J. Kraushaar, and B. W. Ridley, *Bull. Am. Phys. Soc.* **11**, 119 (1966).

²⁸ S. M. Shafroth, P. N. Trehan, and D. M. Van Patter, *Phys. Rev.* **129**, 704 (1963).

²⁹ J. Alster, D. C. Shreve, and R. J. Peterson, *Phys. Rev.* **144**, 999 (1966).

with the expected weak coupling value of 0.67. The angular distributions for the two $L=3$ transitions at 2.20 and 2.51 MeV are also shown in Fig. 11. The ratio of the cross sections of the 2.20-MeV state to that of the 2.51-MeV state is 0.78 ± 0.07 , again in good agreement with the theoretical value of 0.75. The agreement in the case of the $L=2$ states may be fortuitous because of the uncertainties in the experimental cross sections.

The sum of the two He^3 scattering cross sections which correspond to a single state in the Sr^{88} core should be equal to the He^3 cross section for excitation of that

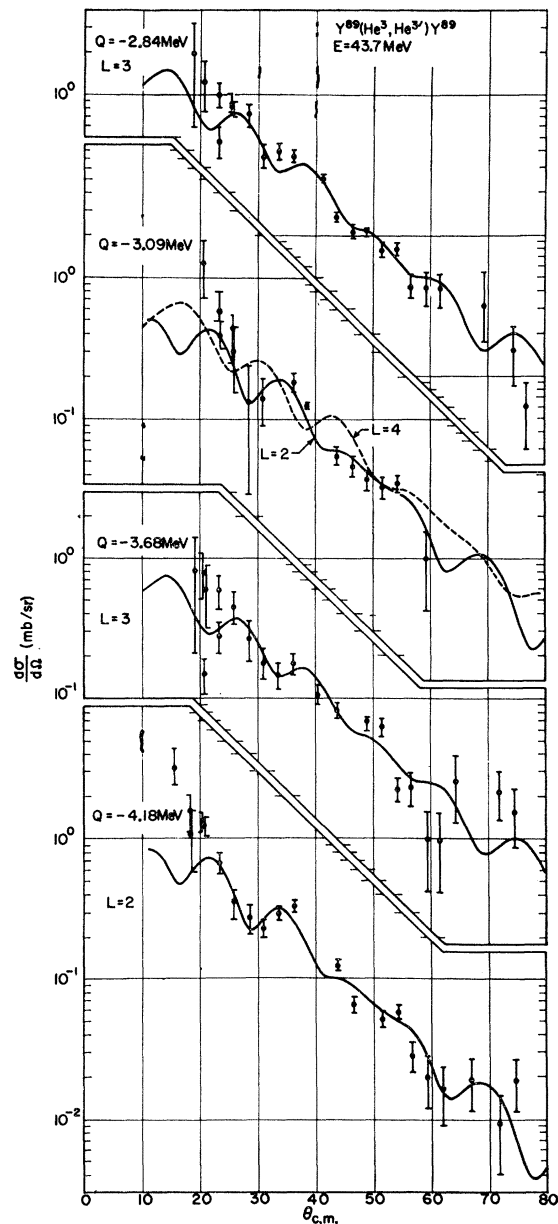


FIG. 12. Experimental and theoretical angular distributions for four higher-lying states in Y^{89} .

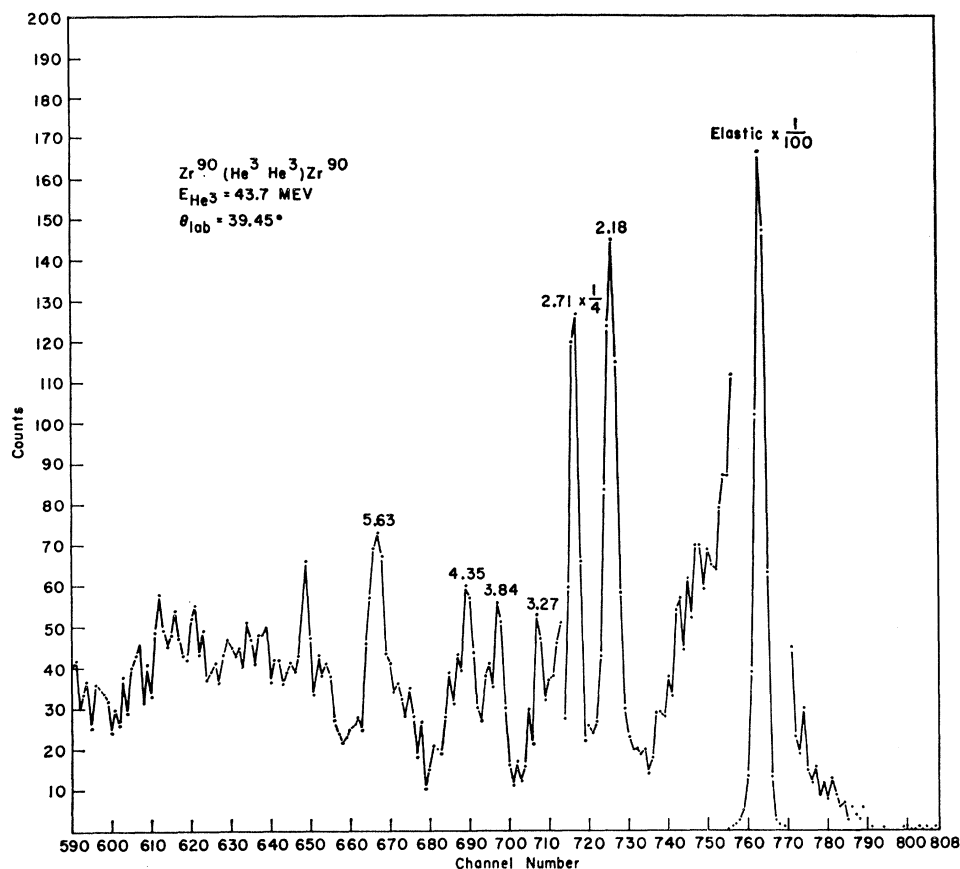


FIG. 13. An energy spectrum of 43.7-MeV He³ ions scattered from Zr⁹⁰.

state in Sr⁸⁸. No He³ scattering has been reported from Sr⁸⁸, so this comparison cannot be made.

The Y⁸⁹ nucleus may alternatively be considered as a Zr⁹⁰ core and a proton hole in the $p_{1/2}$ shell. In this case, the above expression should hold equally well. The results of comparing the center of gravity energy of the Y⁸⁹ multiplets with the energy of the corresponding states in Zr⁹⁰ using the energies derived from the measurements discussed in the next section are summarized in Table III. The agreement is not particularly good for either the 3⁻ or 2⁺ states, but is better for the 3⁻ states.

Comparing the sums of the cross sections for the multiplets with the corresponding Zr⁹⁰ core cross sections at 20° we get the following:

For $L=2$

$$\left. \frac{d\sigma}{d\Omega} \right|_{\text{Zr}^{90}} = 2.3 \pm 0.1 \text{ mb/sr},$$

$$\sum \left. \frac{d\sigma}{d\Omega} \right|_{\text{Y}^{89}} = 1.5 \pm 0.2 \text{ mb/sr}.$$

For $L=3$

$$\left. \frac{d\sigma}{d\Omega} \right|_{\text{Zr}^{90}} = 2.0 \pm 0.1 \text{ mb/sr},$$

$$\sum \left. \frac{d\sigma}{d\Omega} \right|_{\text{Y}^{89}} = 1.45 \pm 0.2 \text{ mb/sr}.$$

The agreement here again is better for the $L=3$ states but is not good for either.

Four additional distributions of He³ inelastically scattered from Y⁸⁹ are shown in Fig. 12. A fair correspondence is obtained between the 2.84- and 3.68-MeV data and predictions for $L=3$ transitions. Though far from conclusive these observations agree with the assignments made from alpha-particle scattering data by Alster *et al.*²⁹ They also find that the 3.08-MeV state corresponds either to an $L=2$ or 4 transition. The angular distribution predicted by the distorted-wave theory for an $L=2$ transition agrees reasonably well with the data, but an $L=4$ distribution is out of phase with the experimental data. The angular distribution for scattering from the state seen at 4.18 MeV also compares reasonably well with an $L=2$ transition. Again this assignment is not conclusive, but is in agreement with Alster's assignment.

TABLE III. The center-of-gravity energy of Y⁸⁹ compared to the core energy in Zr⁹⁰.

	Center-of-gravity energy (MeV)	Core-state energy (MeV)
$E_2 - E_0$	1.58 ± 0.07	2.18
$E_3 - E_0$	2.38 ± 0.07	2.71
$E_3 - E_2$	0.80	0.53

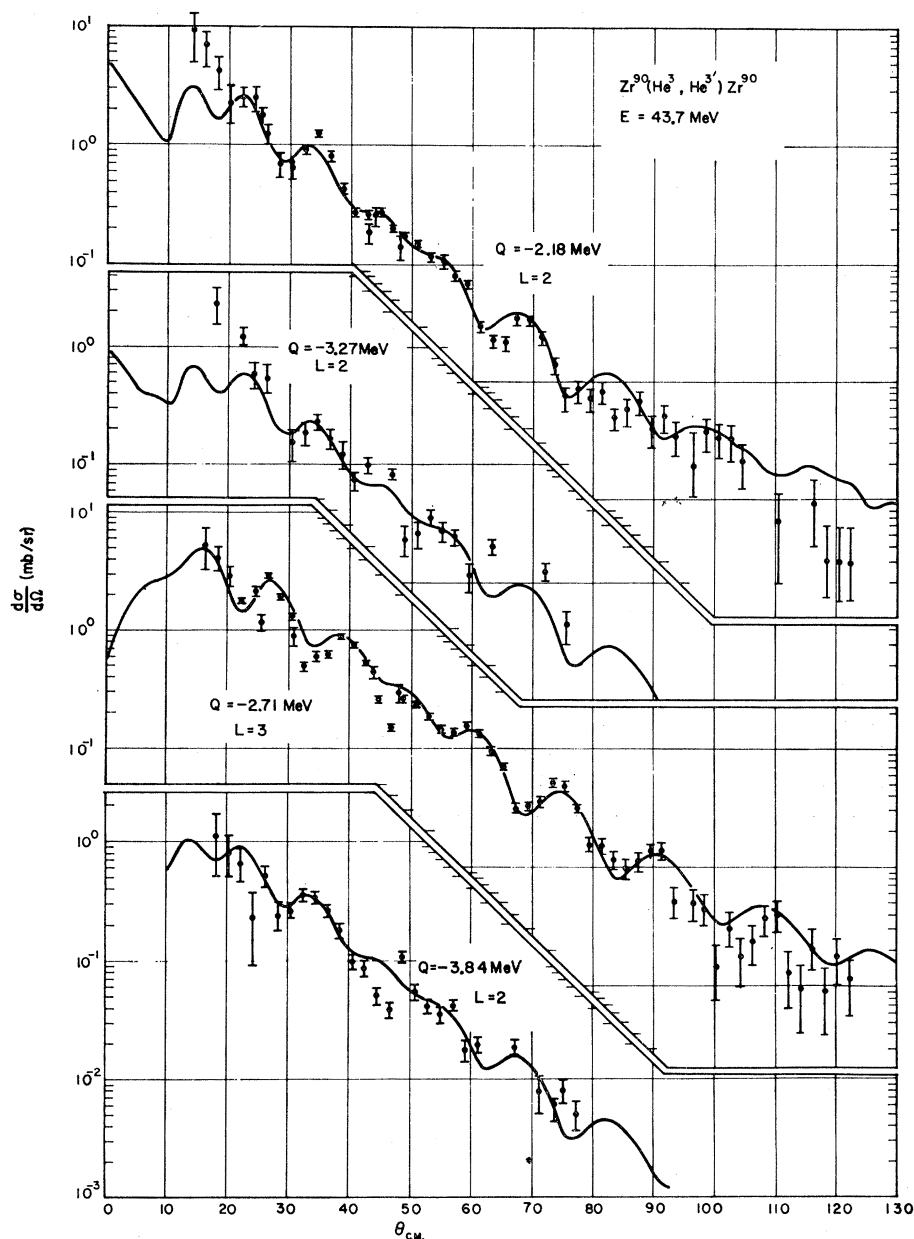


FIG. 14. Experimental and theoretical angular distributions for Zr^{90} .

Inelastic groups were also seen that corresponded to states at 3.99, 4.34, 4.48, 4.76, 5.12, 5.70, and 6.88 MeV, but the angular distributions were too incomplete to be useful.

F. Results from Zr^{90}

Only a few states were seen at enough angles in the He^3 scattering from Zr^{90} to obtain angular distributions for them. All states except the $L=2$ state at 2.18 MeV and the $L=3$ state at 2.71 MeV were weakly excited as can be seen in a typical spectrum, Fig. 13. Noting that the elastic peak is 100 times larger than drawn, the states at 3.27, 3.84, 4.35, and 5.63 MeV are very weak. Evidence for many of the states seen in pro-

ton scattering by Gray *et al.*³⁰ can be seen as small spikes for excitation energies greater than 2.71 MeV. The states at 2.18 and 2.71 MeV were strongly excited and good counting statistics were obtained at most angles less than 100° for scattering corresponding to these two states. The 2.18-MeV state along with the ground state was used to obtain the conversion gain.

In Fig. 14 are shown the angular distributions for the strong states at 2.18 and 2.71 and the somewhat weaker states at 3.27 and 3.84 MeV. The distorted-wave calculations for $L=2$ and $L=3$ transitions using a complex-potential collective-model interaction are drawn with

³⁰ W. S. Gray, R. A. Kenefick, J. J. Kraushaar, and G. R. Satchler, *Phys. Rev.* **142**, 735 (1966).

TABLE IV. Deformation parameters and deformation lengths for the states where the angular-momentum transfer is reasonably certain.

Target	-Q (MeV)	L	β		βR^a		References
			He ³ present	α others	He ³ present	α others	
Ca ⁴⁰	3.73	3	0.23	0.19, 0.24	1.29	0.85, 1.36	15, 17
	4.48	5	0.079	0.077, 0.13	0.44	0.35, 0.73	15, 17
	6.28	3	0.078	0.088, 0.12	0.44	0.40, 0.68	15, 17
	6.59	3	0.062	0.069, 0.09	0.35	0.35, 0.51	15, 17
Fe ⁵⁶	0.85	2	0.21		1.29		
	2.66	2	0.05		0.31		
	4.52	3	0.12		0.74		
Ni ⁵⁸	1.46	2	0.15	0.15-0.19	0.90	0.91-1.05	5, 9, 10
	4.45	3	0.12	0.14-0.18	0.75	0.80-1.11	5, 9
Y ⁸⁹	1.45	2	0.045	0.020	0.32	0.14	29
	1.69	2	0.046	0.028	0.33	0.20	29
	2.20	3	0.069	0.037	0.49	0.26	29
	2.51	3	0.074	0.047	0.53	0.33	29
	2.84	3	0.069	0.034	0.49	0.24	29
	3.68	3	0.051	0.021	0.37	0.19	29
	4.18	2	0.052	0.024	0.37	0.17	29
	4.18	2	0.052	0.024	0.37	0.17	29
Zr ⁹⁰	2.18	2	0.073	0.066	0.52	0.46	31
	2.71	3	0.11	0.12	0.78	0.84	31
	3.84	2	0.047	0.043	0.33	0.30	31

^a For He³ the radius of the imaginary part of the potential has been used.

the 2.18- and 2.71-MeV data, respectively. The calculated distribution for $L=2$ compares very well with the data for the 2.18-MeV state, and deviates from it at only a few angles. The agreement between the $L=3$ distorted-wave angular distribution and the experimental distribution for the 2.71-MeV state is excellent. Judging from the phase and the reasonable agreement of an $L=2$ theoretical curve to the 3.27-MeV state, it may also correspond to an $L=2$ transition. Gray *et al.*,³⁰ using shell-model calculations, assign possible $L=0$ and 2 transitions to this state. This work does not eliminate the possibility of an $L=0$ transition. An $L=2$ distorted-wave curve gives a fair description of the 3.84-MeV distribution, which is the assignment made by Gray *et al.*³⁰ and Bingham *et al.*³¹

IV. DEFORMATION PARAMETERS

The deformation parameters calculated using the distorted-wave theory are listed in Table IV for the states where the angular-momentum transfer seems rather certain. Also shown are deformation lengths, as it has been suggested that βR rather than β should be compared for various measurements. For He³ scattering the interaction radius is not uniquely defined, but it appears clear that the imaginary radius R' should be used since the imaginary term is the dominant one in the interaction. For a comparison, values of β and βR derived from alpha-particle scattering measurements are listed when available. In calculating βR for alpha-particle scattering, the radius is well defined since the

real and imaginary radii were the same for the optical potentials considered.

The deformation parameters from He³ are in reasonable agreement with those from alpha-particle scattering. There does not seem to be any systematic discrepancy except for Y⁸⁹ where the values of β from alpha-particle scattering are smaller by a factor of about 2. The values of βR do not appear appreciably more consistent than do the values of the deformation parameter alone.

Although not shown in Table IV, the deformation parameters were also compared with those from proton scattering. In general, those from proton scattering are somewhat higher, and in particular this is so when only a real interaction has been used in the distorted-wave calculations. In the case of Fe⁵⁶ and Ni⁵⁸ inelastic He³ scattering at 22 MeV has been measured.⁷ The values of β and $\beta R'$ derived from that experiment are in good agreement with the He³ values shown in Table IV for the strong collective transitions.

V. SUMMARY

The inelastic scattering of He³ ions has been found to resemble that of alpha particles with similar center-of-mass momenta. In particular, the angular distributions exhibit well developed oscillatory behavior with phases that are qualitatively, though not precisely, in agreement with the Blair phase rule. The amplitude, however, of the alpha-scattering oscillations appears generally to be greater than those with He³. States that are strongly excited by inelastic scattering of other particles are also strongly excited by He³. Unfortunately,

³¹ C. R. Bingham, M. L. Halpert, and R. H. Bassel, Phys. Rev. 148, 1174 (1966).

no data were obtained for excitation of states with unnatural parity, where one might expect major differences between He^3 and α -particle scattering.

Distorted-wave calculations were carried out for comparison with the more complete angular distributions. These calculations used for, the most part, a collective-model interaction based upon equal deformations of the real and imaginary parts of an optical potential that had been found to fit the elastic scattering. Of several families of such potentials the one with U_0 in the range 170 to 180 MeV was chosen for the distorted-wave calculations because it had been found to provide substantially the best fit to particle-transfer reactions involving He^3 . In some trial calculations, this potential was also found to provide a marginally better fit to inelastic He^3 scattering from the lowest 2^+ and 3^- states of Ni^{58} than did two other "elastic-scattering" potentials with $U_0 \sim 60$ and ~ 120 MeV.

In general, the angular distributions predicted with the deformed complex potential agreed quite well with the data for excitation of states with known spin and parity. The deformation parameters β needed to reproduce the absolute cross sections for even nuclei were also in reasonable accord with the results from scattering of other kinds of particle. In contrast to this, when only the real part of the potential was deformed, the calculated distributions agreed rather poorly in shape with the data, except in the case of the lowest 2^+

state in Fe^{56} . Moreover, the absolute cross sections had only about one-sixth of the magnitude calculated with the complex interaction, resulting in deformation parameters that were two to three times larger than found in other experiments.

The agreement between theory and experiment was most consistently good for the more strongly excited 2^+ , 3^- , and 5^- states. The angular distributions associated with the 4^+ states, were on the whole, less reliably reproduced by the distorted-wave theory. Whether, in the case of the 2.08-MeV state of Fe^{56} and the 2.46-MeV state of Ni^{58} , this was due to multiple phonon excitation or their being unresolved multiplets is not clear. Nevertheless, the higher 4^+ state at 4.72 MeV in Ni^{58} was rather well reproduced by the theory.

The ratio of the cross sections for the first two excited states in Y^{89} corresponding to angular-momentum transfer $L=3$ agrees well with that expected from the weak-coupling, core-excitation model. The cross-section ratio for the two lowest-lying states for $L=2$ also appears to agree with this model, although the cross sections were not good enough to make this agreement conclusive. The spacing of the center of gravities of the multiplets does not agree with that of the core states and the sums of the multiplet cross sections are not equal to the corresponding core cross sections for either $L=3$ or $L=2$ when Y^{89} is considered as a Zr^{90} core and a proton hole. However, the agreement was better for the $L=3$ states than for the $L=2$ states.